# Single- and double-electron capture by 1–100-keV protons in collisions with magnesium and barium atoms

T. J. Morgan and F. J. Eriksen*
*Physics Department, Wesleyan University, Middletown, Connecticut 06457*
(Received 12 October 1978)

Absolute total cross sections for single- and double-electron capture by $H^+$ in collisions with Mg and Ba have been measured for energies between 1 and 100 keV. The single-electron-capture cross section has also been calculated with the Gryzinski formalism of the classical binary-encounter approximation. The measured cross sections exhibit both high- and low-energy structure. The high-energy behavior is in accord with the Brinkman-Kramers results and classical predictions for the energy at which inner-shell capture becomes important. The low-energy behavior is discussed in terms of a molecular picture of the collision. The cross sections are shown to be critically dependent on curve-crossing effects which occur at avoided crossings between potential curves. At low energies the double-electron-capture cross section in Mg shows pronounced structure consistent with a description of the collision in terms of transitions via the intermediate H ($1s$) state. It is shown that this mechanism is not important in Ba, since curve crossings are expected to take place at internuclear separations too large for transitions to occur. A possible explanation for the decrease in single-electron-capture cross section in Ba at low energies is suggested in terms of competition from direct target-excitation collisions. For single-electron capture in Mg, recent low-energy perturbed-stationary-state calculations and high-energy classical-trajectory Monte Carlo calculations by Olson and Liu are in good agreement with experiment. The present classical binary-encounter approximation results for single-electron capture in both Mg and Ba agree with experiment to within a factor of 2 over the entire energy range. Measurements of single- and double-electron capture are also reported for Ar targets. A pronounced second maximum in the double-electron-capture cross section is found.

## I. INTRODUCTION

Electron transfer in heavy-particle collisions has long been of fundamental and practical interest. A substantial amount of theoretical and experimental work has been performed and is summarized in recent reviews.[1-4] Most work has involved gas targets and more recently an increasing number of measurements have been made on alkali metals and atomic hydrogen. However, a detailed physical understanding of single-electron transfer is not yet available and much less is known about the process of double-electron transfer in a single collision.

One particular class of collision targets—alkaline-earth metal vapors (Mg, Ca, Sr, Ba)—have received very limited attention. Except for Mg we are aware of no previous experimental or theoretical cross-section information. There are several reasons for this void. From an experimental point of view studies of collisions using alkaline-earth vapor targets have been very limited since their chemical activity and physical properties introduce experimental difficulties associated with production and use of the vapors. From a theoretical point of view alkaline-earth atoms are quite interesting. They contain two outer electrons ($ns^2$) and are heliumlike atoms which exhibit strong configuration mixing. These properties make the study of two-electron atoms an important topic in atomic physics but lead to difficulties when trying to model the collision. The problem of two active electrons is particularly complicated and computationally difficult. Accurate representation of the very complex electronic wave functions is a problem. The use of hydrogenlike wave functions to simulate target electrons has severe limitations and further, the effective charge concept is not always suitable for heavy targets. Although somewhat better, Hartree-Fock wave functions still only account for average electron properties. However, it should be noted that recent work on determining accurate ground-state heliumlike wave functions is encouraging.[5] At high energies core effects play an important role in electron transfer collisions and must be taken into account by treating the core and active electrons equally. At low energies, the collision is complicated to model since the low ionization potential of alkaline-earth atoms results in many molecular potential energy crossings between incident and final collision channels.

The present study has been motivated by several recent developments. New theoretical studies on single- and double-electron transfer in proton-magnesium collisions have been carried out by Olson and Liu[6] and work is in progress by others. Also, extrapolations based on trends in known cross sections indicate that barium may be a very attractive charge-exchange target for producing

 

negative hydrogen ions.[7] The need for collisional information on the production of both neutral hydrogen and its negative ion are of current interest for neutral beam injection into fusion plasma devices[8] and in ion source development for high-energy accelerators and storage rings.[9] Finally, recent experimental results indicate that the barium laser is one of the most promising pulsed lasers in the near infrared.[10]

In this paper we report absolute measurements of the total single- and double-electron capture cross section for proton collisions with magnesium and barium atoms. In addition, we present the results of a calculation based on the classical binary-encounter approximation for single-electron capture. We have also studied capture into the metastable $2s$ state of hydrogen from magnesium and barium atoms and this topic is the subject of a separate paper.[11] The energy range of the present study is 1–100 keV. This range includes (i) the low-energy region where a quasimolecular picture of the collision is appropriate and molecular level crossings associated with the evolution of potential states of the collision system play a critical part in the dynamics of the collision; and (ii) the high-energy region where core-electron effects contribute in an important way to the electron transfer process. These features cannot of course be explained within the rubric of a three-body model and may be expected to lead to structure in the total cross section at both high and low energies. Indeed, interesting structure, which can be attributed to the multielectron nature of the alkaline-earth atoms, is observed in the cross sections measured in the present work. The structure is discussed in terms of a molecular picture at low energies and in terms of inner-shell core effects at high energies. We have also carried out measurements in argon and found two pronounced maxima in the double-electron capture cross section.

The results of this study help to fill the gap in our knowledge of electron transfer collisions and serve to test the range of validity of recent low-energy Landau-Zener and perturbed-stationary-state calculations and high-energy classical trajectory Monte Carlo calculations[6] as well as the present binary-encounter approximation calculations.

Extensive theoretical work on electron capture has been carried out for the $H^+ + H$ collision which serves as a prototype in the formulation of scattering theories. Experimental data on more complex atoms over a wide range of energies are required to test the limits of application of existing models. It is hoped that the present results will help meet this need and stimulate further theoretical work on asymmetric charge transfer involving targets with two active electrons surrounding a closed-shell structure.

## II. APPARATUS AND PROCEDURE

### A. General description

A schematic diagram of the apparatus is shown in Fig. 1. $H^+$ ions were produced in a radio-frequency ion source. The ions were extracted from the source and focused with an electrostatic gap-lens assembly. After passing through a four-element accelerating column, the ions reached the desired energy. The beam was electrostatically steered into a 20° bending magnet and passed through a trimming magnetic field and a final set of horizontal and vertical steering plates before entering the target chamber. The beam was collimated by several apertures between the accelerating column and the target. After the target, the beam was charge separated by an electric field and the ion components measured with Faraday cups while the neutral component was measured with a secondary emission detector. (As shown in Fig. 1, the apparatus also contains a Stark quench region and a solar blind channeltron which were used in our study of electron capture into the $n=2$ state.[11]) The apparatus was evacuated by four diffusion pumps. Ambient pressures with the target cell hot were typically $5\times10^{-7}$ Torr in the target region and $2\times10^{-7}$ Torr in the detector re-

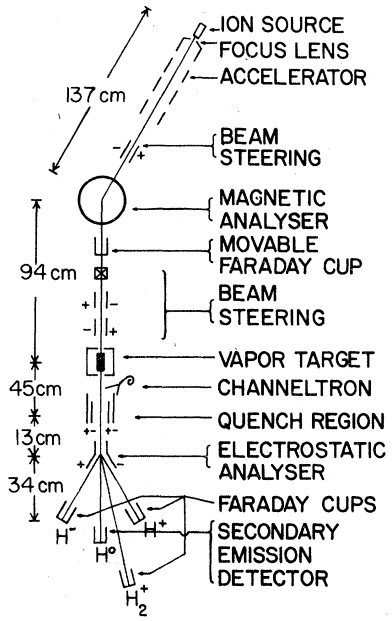


FIG. 1. Schematic diagram of the apparatus. The channeltron and quench region were used in our study of the formation of H (2 $s$) atoms (Ref. 11).

gion. With no vapor in the target cell the background neutral component of the primary $H^+$ beam was always less than 1%. The beam energy was measured with an electrostatic voltmeter calibrated by the National Bureau of Standards. For radio-frequency ion sources the mean ion energy can be up to 400 eV higher than the extraction voltage due to the existence of a plasma sheath.[12] To account for this plasma potential an *in situ* energy analysis of the beam was performed. A three-element retarding field energy analyzer, based on a design of Hopman *et al.*,[13] was constructed and installed in the detection region. A careful study of the beam energy as a function of accelerator voltage and ion source operating parameters was performed. For a given accelerator voltage changes of up to 200 V in the beam energy were observed for different ion source operating conditions used in the present experiment, and were reproducible to within about ±15%. Under typical conditions the beam energy spread was measured to be less than 80 eV and the energy of the beam was known to within ±100 eV based on uncertainties associated with the energy analyzer.

### B. Scattering target

The scattering target cell used in the present experiment is shown in Fig. 2. The cell is made of stainless steel and could be used as a conventional gas target or as a metal-vapor target. The beam entered the cell through a 1-mm diam. aperture attached to a stainless-steel tube which protrudes from the cell. A similar tubular arrangement existed at the 3-mm diam. exit aperture. The purpose of the tubes is to allow for auxiliary heating to the apertures in order to prevent clogging of the holes by vapor condensation. The tubes were heated by passing a current through a tantalum wire wrapped around the tubes. This arrangement is particularly desirable for multiple-collision studies where the pressure in the cell may be up to three orders of magnitude greater than under thin target conditions. (We are presently carrying out multiple-collision experiments in alkaline-earth vapors.[14]) The effective target length of the cell is 5.5 cm and was obtained by adding a small correction to the geometrical length to account for an assumed linear pressure drop through the tubes. The correction due to the finite size of the apertures is negligible since, under present molecular flow conditions, the reduction in density inside the target near the apertures approximately cancels the increase in density outside the apertures. As a check on our apparatus and experimental technique we measured the single- and double-electron capture cross sections,

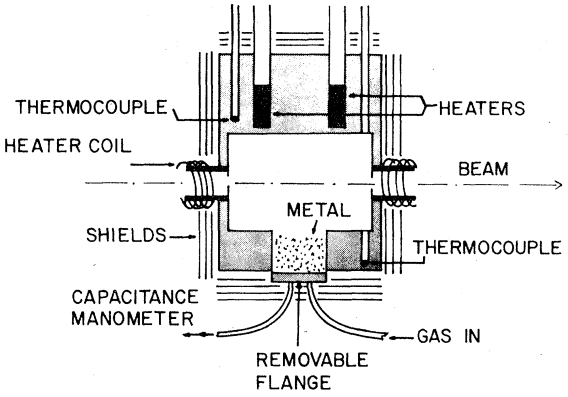


FIG. 2. Scattering target cell (not to scale). The flange containing the gas-in and pressure measuring lines was replaced by a blank flange when the cell was used as a metal-vapor target.

$\sigma_{10}$ and $\sigma_{1-1}$, in argon gas. When used as a gas cell, a gas inlet line and pressure measuring line are connected to the target cell through a mini-conflat flange at the bottom (see Fig. 2). The gas target pressure was measured with a capacitance manometer with the gauge mounted on a thermostatically controlled heater to improve stability and reduce the effects of ambient temperature variations. Cross sections in argon were measured for both cold and hot targets and the data were found to be independent of the cell temperature.

The cell was heated by two 150-W resistive heating elements which were press fit into holes in the cell cylinder. When used as a metal-vapor oven a blank flange replaced the one shown in Fig. 2. In this case a stainless-steel gasket was used to make the seal since it was found that copper reacts with barium at high temperature. The oven and the tubular apertures were surrounded by a layered stainless-steel heat shield. Two chromel-alumel thermocouples, one above the beam line and one below, served to measure the temperature of the cell. Data were taken under conditions in which the two thermocouples read essentially the same temperature. The thermocouples were calibrated at 273 K, 373 K, and *in situ* by observing the melting plateau of a temperature versus time plot (with constant power in the heaters) for lead at 600.7 K. As a result of these tests we estimate the uncertainty in temperature to be ±2 K. Data were taken for oven temperatures from 580 to 680 K for magnesium (99.99%) and from 720 to 870 K for barium (99.99%). Care was taken to outgas the oven at temperatures considerably higher than operating temperatures for several hours before data were taken. Values of vapor pressure as a function of oven temperature were obtained

from a curve fitted to the available data points given by Hultgren *et al.*[15]

### C. Detection region

The detector region consisted of a 1-m diam., 0.3-m deep stainless-steel chamber pumped by a liquid-nitrogen trapped diffusion pump. The chamber contained a set of angled plates for beam charge analysis, two Faraday cups, and a secondary emission detector. Care was taken to ensure that the beam components intercepted the center of the detectors. Beam profiles obtained by scanning the charged beams across the Faraday cups demonstrated a well resolved plateau. The entire apparatus was aligned with the aid of a laser located before the bending magnet. The target and neutral detector were positioned such that laser light passed through the magnet and target and intercepted the center of the in-line secondary emission detector.

An important consideration in low-energy absolute cross-section measurements is to ensure complete collection of the scattered beam. This was experimentally demonstrated by changing the angular acceptance of the detectors and measuring the cross sections for a 2-keV $D^+$ incident beam (the lowest energy used in the present experiment). Cross sections were measured for half-angle acceptances of 25, 18, and 15 mrad with no observable differences in the data. Most of the data reported were taken with a half-angle acceptance of 18 mrad. The Faraday cups were designed to ensure complete electrostatic suppression of secondary electrons. Typical suppression voltages of 200 V were applied and a plateau in the signal was clearly evident. The secondary emission detector consisted of a grounded stainless-steel disk surrounded by a positively biased cylinder to collect secondary electrons. Complete collection was experimentally verified. The number of secondary electrons per incident proton $\gamma^+$ was measured several times during a run and the relation $\gamma^0/\gamma^+ = 1.11$ was used to determine the secondary emission coefficient $\gamma^0$ for hydrogen atoms. This relation has been verified down to 1.5 keV by Pradel *et al.*[16] and recently demonstrated to hold for energies well below 1.0 keV.[17] The use of this relation in the present experiment assumes that $\gamma^0/\gamma^+$ is independent of target surface and angle of incidence of the beam.

## III. DATA ACQUISITION AND ANALYSIS

The fraction of the total beam in a particular charge state $k$, $F_k$, is related to the target thickness $\pi = nL$, where $n$ is the target density and $L$ is the effective target length, by the coupled differential equations

$$\frac{dF_k}{d\pi} = \sum_{j \neq k} (F_j \sigma_{jk} - F_k \sigma_{kj}) \quad j, k = 1, 0, -1. \tag{1}$$

The solution, under thin-target–single-collision conditions (first-order solution in $\pi$), for a beam initially in charge state $j$ is

$$F_k = \sigma_{jk} \pi. \tag{2}$$

The cross section $\sigma_{10}$ and $\sigma_{1-1}$, for the capture of one and two electrons, respectively, can therefore be obtained from the slope of the experimental data for the neutral and negative ion fractions as a function of target thickness. Figure 3 shows typical data taken during the course of the present experiment. The lines represent a least-squares fit to the data. Although simple in approach, this method can lead to errors if single-collision conditions are not truly satisfied. It has recently been demonstrated[18] that experimental verification of linearity between $F_k$ and $\pi$ may not necessarily provide a sensitive enough test to guarantee single-collision conditions if competing secondary cross sections are large. Over the present energy range, collision cross sections vary by several orders of magnitude and care must be taken to estimate their effects and, where appropriate, make corrections to the first-order solution; even for small values of $\pi$. (The range of $\pi$ used in the present experiment was 0.5 to $8 \times 10^{13}$ cm$^{-2}$). In the case of Mg, cross sections for competing processes are known[19] and where necessary corrections to the data were made. The largest correction was ~15% and occurred in $\sigma_{1-1}$ at high energies. This is due to the fact that at the higher energies of the present experiment $\sigma_{-10}$ is almost five orders of magnitude

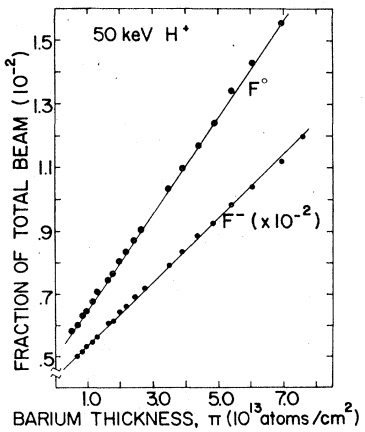


FIG. 3. Measured $H^0$ and $H^-$ fractions as a function of Ba target thickness for a 50-keV $H^+$ beam. The lines represent a least-squares fit to the data and were used to determine the slope.

greater than $\sigma_{1,-1}$. Since competing collision cross sections are not available for Ba, estimates of the corrections were made based on extrapolations of the Mg results. This procedure introduced additional uncertainties in our $\sigma_{1,-1}$ cross section in Ba at high energies. Assigned relative uncertainties are based on these second-order correction effects, as well as on reproducibility of the data over a period of several months (±10%) and on our knowledge of the effective target length (±3%). The uncertainty in the energy is negligible except at low energies where it reaches ±10% due to an uncertainty in the primary beam energy of ±100 eV. A systematic uncertainty of ±20% is also assigned to the data based on knowledge of the vapor pressure (see Ref. 15).

## IV. RESULTS AND DISCUSSION

The present results for single- and double-electron capture in argon gas are shown in Fig. 4 together with previous data of Stier and Barnett[20] and Williams.[21] Ar measurements were undertaken in order to check our apparatus and experimental technique, and to investigate the low-energy behavior of the double-electron capture cross section $\sigma_{1,-1}$. The study of $\sigma_{1,-1}$ at low energies was motivated by recent results in xenon gas which showed a pronounced second maximum in $\sigma_{1,-1}$ at about 3 keV.[22] Although earlier measurements had indicated structure in $\sigma_{1,-1}$ for both Ar and Xe the results of Morgan *et al.*[22] showed that the low-energy maximum in Xe is a factor of 2 larger than previously reported. The present results show that the low-energy maximum in Ar is approximately a factor of 2 larger than previously reported. For energies greater than 10 keV the recent $\sigma_{1,-1}$ results in Xe and the present $\sigma_{1,-1}$ results in Ar agree with earlier measurements. The present results for $\sigma_{10}$ in Ar are in good agreement with the measurements of Stier and Barnett over the entire energy range. The data for Ar were taken with both cold and hot targets and with $H^+$ and $D^+$ incident ions. Neither a cell temperature effect nor an isotope effect were observed.

The single-electron-capture cross section in Mg is shown in Fig. 5. The present results are in general agreement with previous experiments.[19,23,24] A classical impact-parameter calculation[25] and Brinkman-Kramers (BK) calculations[26] in both the prior and post approximations using hydrogenlike and Hartree-Fock wave functions have been performed. The results of these calculations show a maximum at about the right energy but lie well above the data and have not been included in Fig. 5. Two semiempirical prescriptions for adjusting BK results for complex atoms have been suggested by Mapleton[19] and Nikolaev[27] and applied to Mg by Berkner *et al.*[19] (curves *M* and *N* in Fig. 5). Both prescriptions improve the BK results significantly but fail to accurately reproduce the experimental data at high and low energies. At low energies, where the character of the collision is molecular, BK semiempirical adjustments are not expected to give quantitatively accurate results. At high energies the disagreement cannot be explicitly attributed to the neglect of inner-

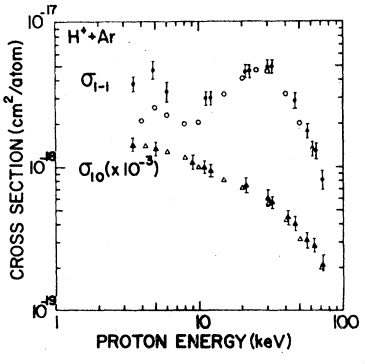


FIG. 4. Single- and double-electron capture cross sections $\sigma_{10}$, $\sigma_{1,-1}$ for collisions of $H^+$ with Ar. $\sigma_{10}$: ▲, present data; △, Stier and Barnett (Ref. 20). $\sigma_{1,-1}$: ●, present data; ○, Williams (Ref. 21).

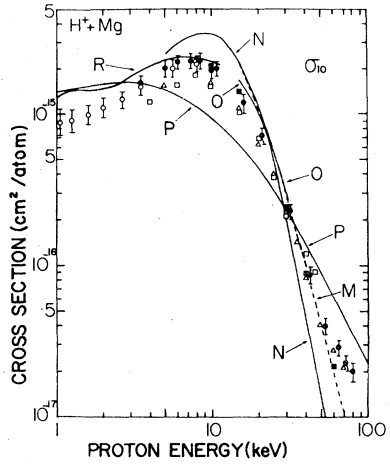


FIG. 5. Single-electron-capture cross section $\sigma_{10}$ for collisions of $H^+$ with Mg. ●, present data using $H^+$ ions; ○, present data using $D^+$ ions; △, Berkner *et al.* (Ref. 19); □, Futch and Moses (Ref. 23); ■, Il'in *et al.* (Ref. 24); curve *P*, present Gryzinski calculation; curve *R*, perturbed-stationary-state calculation of Olson and Liu (Ref. 6); curve *O*, classical Monte Carlo calculation of Olson and Liu (Ref. 6); curve *N*, Nikolaev's semiempirical prescription (Ref. 19); curve *M*, Mapleton's semiempirical prescription (Ref. 19). The cross sections for $D^+$ ions have been plotted at ½ the $D^+$ energy.

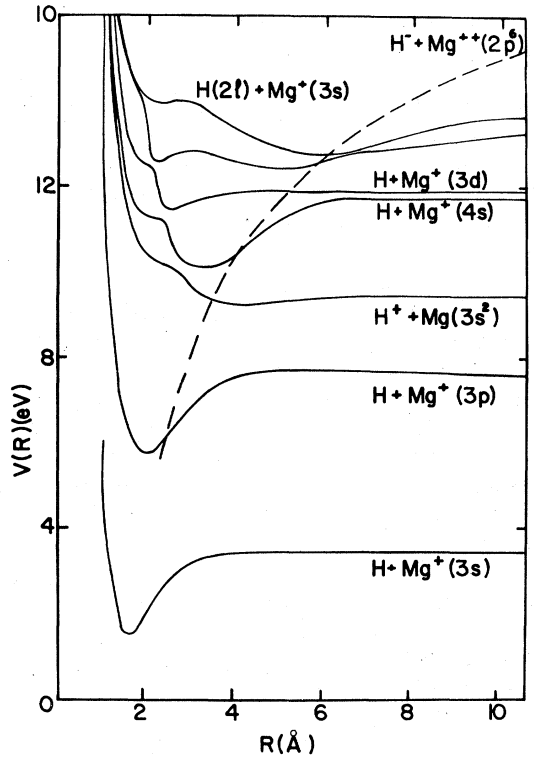


FIG. 6. Potential energy $V(R)$ for the $HMg^+$ system as a function of internuclear separation $R$. Solid lines denote *ab initio* configuration interaction potential energy curves of Olson and Liu (Ref. 6). The dashed line represents an estimate of the $H^-+Mg^{2+}$ system determined from known energy values at infinite separation added to a $-2e^2/R$ term.

electron charge exchange in the calculation since capture of $3s^2$, $2p^6$, and $2s^2$ electrons of magnesium were included. The curves in Fig. 5 labeled $R$ and $O$ are the recent theoretical results of Olson and Liu.[6] Curve $O$ is the result of a classical trajectory Monte Carlo method. The cross sections are obtained from a numerical solution to the coupled Hamilton's equations of motion subject to random initial conditions. The results of this calculation are in good agreement with the present experimental data and extrapolate well to low energies. The low-energy cross sections (curve $R$) were derived from *ab initio* calculations of the $HMg^+$ potential-energy curves using a two-state close-coupling method and perturbed-stationary-state calculation with straight-line trajectories. Figure 6 shows the *ab initio* potential energy curves derived by Olson and Liu and used by them, with $H(1s)+Mg^+(3p)$ as the post collision channel, to obtain curve $R$ in Fig. 5. The cross section is estimated to be accurate to within approximately 40%. Since the calculation does not allow for loss of flux to the excitation and double-charge-transfer channels the results are expected to be slightly higher than the experimental single-electron capture cross section. It can be seen from Fig. 5 that the agreement between the low-energy calculation (curve $R$) and the present measurements is within the combined theoretical and experimental uncertainties. The high-energy maximum in $\sigma_{10}$ is reproduced well by the theory. The experimental results indicate that the structure below 2 keV, although present is not as pronounced as predicted. Curve $P$ in Fig. 5 is the result of the present calculation for single-electron capture into $n=1$ and $n=2$ states of hydrogen using the Gryzinski formalism of the binary-encounter approximation.[28] Gryzinski's classical expression for the cross section $\sigma_c$ for single-electron capture from a subshell of the target in the process $B^+ + A \rightarrow B + A^+$ can be written[29]

$$\sigma_c = (\sigma_0 N_e)(U_B/U_A^3)G(U_B/U_A; v_B/v_A);$$

where

$$G(U_B/U_A; v_B/v_A) = \frac{F(v_B/v_A)}{[1+(v_B/v_A)^2]^2 - (U_B/U_A)^2}, \tag{3}$$

and

$$F(v_B/v_A) = (v_A/v_B)^2[v_B^2/(v_B^2+v_A^2)]^{3/2}.$$

In this expression $N_e$ is the number of equivalent electrons for capture from the subshell of the target, $U_A$ and $U_B$ are the binding energies of the electron before and after the collision,[30] $v_A$ is the velocity of the electron in the target atom, $v_B$ is the velocity of the incident ion and $\sigma_0 = 1.312\times10^{-13}$ $eV^2\,cm^2$. The total electron-capture cross section $\sigma_{10}$ is obtained by summing the cross section for each subshell.

As can be seen from expression (3) the cross section diverges for some $v_B > 0$ when $U_A < U_B$. This occurs at an incident ion energy

$$E = (M_B/m)(U_B - U_A), \tag{4}$$

where $m$ is the mass of the electron and $M_B$ is the mass of the incident ion. In obtaining Eq. (4) and in the calculations for the cross sections we have used the relation $v_A = (2U_A/m)^{1/2}$ which is valid for a central force field and is consistent with the present classical approach. For capture into $n=2$ states in Mg, $U_A > U_B$. However, for capture into the $1s$ state $U_A < U_B$ and the cross section diverges at $E = 10.8$ keV. In this case the cross section can still be calculated using expression (3) via detailed balance[31] for the reverse reaction

$$Mg^+(^2S_{1/2}) + H(1s) \rightarrow Mg(^1S_0) + H^+ \tag{5}$$

at equal ion velocity. The calculated cross section for the above collision has been multiplied by

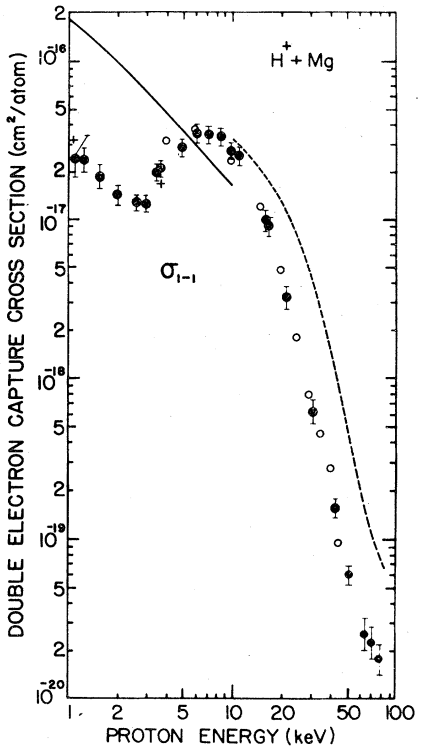


FIG. 7. Double-electron capture cross section $\sigma_{1-1}$ for collisions of $H^+$ with Mg. ●, present data using both $H^+$ and $D^+$ ions; ○, Futch and Moses (Ref. 23); dashed curve, experimental data of Il'in *et al.* (Ref. 33); +, Landau-Zener calculation of Olson and Liu using *ab initio* potential energy curves (Ref. 6); solid curve, Landau-Zener calculation of Olson and Liu using constant potential energy curves (Ref. 34). The cross sections for $D^+$ ions have been plotted at $\frac{1}{2}$ the $D^+$ energy. An isotope effect was not observed.

4 to take into account the number of equivalent target electrons available for capture.

Curve $P$ in Fig. 5 is the sum of the cross sections for capture into $n=2$ states computed directly from expression (3), and into the $n=1$ state computed from expression (3) using detailed balancing. The cross section includes contributions from the $3s^2$, $3p^6$, and $2s^2$ subshells of Mg. As can be seen from Fig. 5 the results of the calculation agree with the present experimental data to within a factor of 2 over the entire energy range. Similar agreement is found in the case of Ba (see below). Based on the present results we expect the model to predict $\sigma_{10}$ to within a factor of 2 or 3 for $H^+$ collisions with other alkaline-earth targets and perhaps for other collisions which have similar internal energy balance.

In Fig. 7 we present results[32] for the double-electron capture cross section in Mg together with previous experimental[23,33] and theoretical[6,34] data. The presence of Coulomb attraction in the post-collision channel distinguishes this collision process from the more extensively studied single-electron capture process. The shape of the cross section—a sharp high-energy maximum followed by a pronounced rise in the cross section at low energy—suggests two distinct mechanisms are important in determining the double-electron capture process in Mg. The structure in the cross section is similar to that found in Ar (see Fig. 4) and in Xe.[22] A survey of the literature shows that structure of this kind is not present in proton collisions with simple molecules or alkali-metal atoms. A complete explanation of the two mechanisms involved in the formation of $H^-$ requires a careful study of the molecular potential energy curves of the collision system and a determination of the strength of the coupling matrix elements associated with avoided crossings of the molecular states during the collision. In the case of double-electron capture in Mg, it has been suggested[6] that the high-energy maximum is due to the incoming $H^+ + Mg(3s^2)$ channel passing diabatically through the series of curve crossings on the inward portion of the trajectory and interacting with the $H^- + Mg^{2+}$ channel on the repulsive wall of the potentials. The low-energy behavior is attributed to an avoided crossing between the $H^+ + Mg(3s^2)$ channel and the $H + Mg^+(4s)$ channel on the outward portion of the trajectory, followed by a series of curve crossings which lead the attractive Coulomb potential out to the $H^- + Mg^{2+}$ products. Assuming the avoided crossings at 2.9 and at 5.8 Å are the low energy $H^-$ rate determining transitions, Olson and Liu[6] have performed a crude Landau-Zener calculation for $\sigma_{1-1}$ and good agreement is found with the present measurements (see Fig. 7).

The present results for single- and double-electron capture in barium are shown in Fig. 8. We are aware of no previous experimental or theoretical data for this collision. Furthermore, we are not aware of any potential energy curves for $HBa^+$. The set of likely single-electron exchange channels in Ba is much more complex than in Mg. For $H^+ + Mg$ collisions there are only two exothermic charge exchange states lying below the initial state. In the case of Ba, there are seven $H(1s) + Ba^+(ns, np)$ states and many more $H(1s) + Ba^+(nl; l > 1)$ states below the initial state. In addition, several of these states are within 1 eV of the initial state. Based on simple energy balance arguments it would appear that $\sigma_{10}$ in Ba should exhibit near-resonant behavior, i.e., reach a rather large maximum value at an energy well below the present range. The present results do not support this expectation (see Fig. 8) down to 2 keV. The maximum value of the cross section is only 30% higher than in Mg and occurs at about 4.5 keV. Since

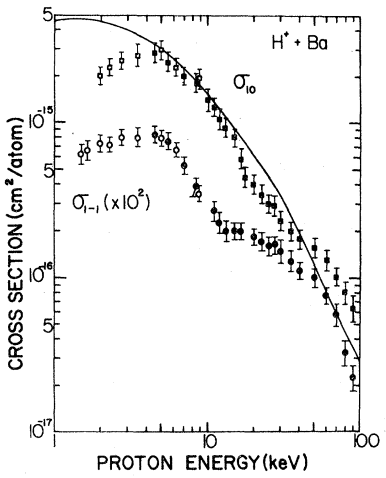


FIG. 8. Single- and double-electron capture cross sections $\sigma_{10}$, $\sigma_{1-1}$ for collisions of $H^+$ with Ba. $\sigma_{10}$: ■, present data using $H^+$ ions; □, present data using $D^+$ ions; solid curve, present Gryzinski calculations. $\sigma_{1-1}$: ●, present data using $H^+$ ions; ○, present data using $D^+$ ions. The cross sections for $D^+$ ions have been plotted at $\frac{1}{2}$ the $D^+$ energy.

there are several $H^+ + Ba^*$ excitation states about 1 eV above the initial state it may be that at low energies, the competing process of direct target excitation without charge transfer dominates the collision. The other competing process, that of double-electron capture, is negligible based on the present measurements.

The solid curve in Fig. 8 is the present result for $\sigma_{10}$ based on the Gryzinski formalism of the binary-encounter approximation.[28] The calculation was carried out in the same manner as for Mg (see above) and includes capture from the $6s^2$, $5p^6$, $5s^2$, and $4d^{10}$ subshells of Ba. A factor of 2 agreement is found with experiment over the present energy range.

At low energies the magnitude of $\sigma_{1-1}$ in Ba is small in comparison to Mg. Based on a simple Coulomb approximation for the potential energy curves at large internuclear separations $R$, i.e., the potential energy of the $H^- + Mg^{2+}(Ba^{2+})$ system is $-2e^2/R$ and the potential energy of the ion-plus-neutral system is constant, the crossing between the initial state and the final Coulomb state occurs at an internuclear separation

$$R_x = 28.8/\Delta E_\infty \text{ Å} \qquad (6)$$

where $\Delta E_\infty$ is the energy defect of the states at infinite separation in eV. For Mg, $\Delta E_\infty = 8.2$ eV and $R_x \simeq 3.5$ Å. For Ba, $\Delta E_\infty = 0.7$ eV and $R_x \simeq 41$ Å. At such large $HBa^+$ separations coupling matrix elements are small and the crossing will be traversed diabatically. The important difference between low-energy $H^-$ formation in Mg and Ba is that in the case of Ba the Coulomb potential crosses collision states at large separations for which transitions are unlikely. In contrast, the crossings in Mg are at reasonable separations for transitions to occur (see Fig. 6).

The high-energy structure in $\sigma_{10}$ and $\sigma_{1-1}$ in both Mg and Ba can be discussed in terms of inner-electron core contributions to the capture process. Hiskes[26] has performed BK calculations which clearly show that capture from the $n=2$ shell of Mg becomes important at 50 keV. As can be seen from Figs. 5 and 7 both $\sigma_{10}$ and $\sigma_{1-1}$ begin to decrease less steeply with energy at ~50 keV. A semilog plot of the data clearly shows the change in energy dependence. Further evidence for high-energy inner-shell capture in $H^+$ collisions with complex atoms is seen in the recent $\sigma_{10}$ measurements of Meyer and Anderson.[35] Their data for $H^+ + Cs$ collisions show a distinct change in energy dependence at ~15 keV; in agreement with BK predictions[36] of a significant $5p^6$ core contribution at 20 keV. As can be seen from Fig. 8 both $\sigma_{10}$ and $\sigma_{1-1}$ in Ba exhibit structure in the energy range 15–40 keV. In contrast, the Ar data for $\sigma_{10}$ (see Fig. 4) do not exhibit high-energy structure in accordance with BK predictions[36] that inner-shell contributions are not important below about 300 keV in inert gases. It should also be mentioned that the modified classical theory of Thomas is in good agreement with BK predictions for the onset of inner-shell capture in Mg and Ar.[25] Finally, a comparison of the magnitude of both $\sigma_{10}$ and $\sigma_{1-1}$ in Ba and Mg clearly shows the effect of inner-shell capture. For example, although $\sigma_{1-1}$ in Mg is larger than $\sigma_{1-1}$ in Ba for $E < 25$ keV, at 80 keV $\sigma_{1-1}$ in Ba is more than a factor of 10 larger than $\sigma_{1-1}$ in Mg.

## ACKNOWLEDGMENTS

We take pleasure in thanking Dr. R. E. Olson for helpful discussion and for making available his results prior to publication. The help of M. Mayo and D. Mariani during the acquisition and reduction of data is appreciated. We are indebted to D. Young for his assistance in the construction and assembly of the apparatus. We also thank J. H. Morgan for her aid in carrying out the Gryzinski calculations. This research was sponsored by the U. S. Department of Energy and by Research Corporation.

*Present address: Dept. of Physics, University of Southern Mississippi, Hattiesburg, Miss. 39401.
[1]H. Tawara and A. Russek, Rev. Mod. Phys. 45, 1788 (1973).
[2]B. L. Moiseiwitsch, Rep. Prog. Phys. 40, 843 (1977).
[3]D. R. Bates, Phys. Rep. Phys. Lett. C 35, 306 (1978).
[4]D. Basu, S. C. Mukherjee, and D. P. Sural, Phys. Rep. Phys. Lett. C 42, 146 (1978).
[5]S. G. Lie, Y. Nogami, and M. A. Preston, Phys. Rev. A 18, 787 (1978).
[6]R. E. Olson and B. Liu (private communication).
[7]J. R. Hiskes, Lawrence Livermore Laboratory Report No. UCIR-853 (1976).
[8]*Proceedings of the Symposium on the Production and Neutralization of Negative Hydrogen Ions and Beams*, edited by K. Prelec (Brookhaven National Laboratory, 1977), Report No. BNL 50727.
[9]K. Prelec and T. Sluyters, Rev. Sci. Instrum. 44, 1451 (1973).
[10]P. A. Bokhan and V. I. Solomonou, Kvant. Elektron. (Moscow) 52, 319 (1978) (in Russian).
[11]T. J. Morgan and F. J. Eriksen, Phys. Rev. A (to be published); Bull. Am. Phys. Soc. 23, 1095 (1978).
[12]J. E. Bayfield, Phys. Rev. 182, 115 (1969).
[13]H. J. Hopman, B. Jurgens, J. H. A. van Wakeren, and H. G. Ficke, J. Phys. E 10, 287 (1977).
[14]T. J. Morgan, J. Stone, M. Mayo, and J. Kurose, Bull. Am. Phys. Soc. 23, 1108 (1978).
[15]R. R. Hultgren, P. D. Dlsai, D. T. Hawkins, M. Gleiser, K. K. Kelly, and D. D. Wagman, *Selected Values of Thermodynamic Properties of the Elements* (American Society for Metals, Cleveland, Ohio, 1973).
[16]P. Pradel, F. Roussel, A. S. Schlacter, G. Spiess, and A. Valance, Phys. Rev. A 10, 797 (1974).
[17]F. W. Meyer and C. F. Barnett (private communication).
[18]B. Hird and H. C. Suk, Phys. Rev. A 14, 928 (1976).
[19]K. H. Berkner, R. V. Pyle, and J. W. Stearns, Phys. Rev. 178, 248 (1969).
[20]P. M. Stier and C. F. Barnett, Phys. Rev. 103, 896 (1956).
[21]J. F. Williams, Phys. Rev. 150, 7 (1966).
[22]T. J. Morgan, K. H. Berkner, R. V. Pyle, and J. W. Stearns, in *Electronic and Atomic Collisions*, edited by J. S. Risley and R. Geballe (University of Washington, Seattle, 1975), p. 165; T. J. Morgan, K. H. Berkner, W. C. Graham, R. V. Pyle, and J. W. Stearns, Phys. Rev. A 14, 664 (1976).
[23]A. H. Futch, Jr. and K. G. Moses, in *Abstracts of Papers of the Fifth International Conference on the Physics of Electronic and Atomic Collisions*, edited by I. P. Flaks and E. S. Solov'ev (Nanka, Leningrad, 1967), p. 12. The values given in this reference have been multiplied by 0.81 to take account of the new thermodynamic evaluation given in Ref. 15.
[24]R. N. Il'in, V. A. Oparin, E. S. Solov'ev, and N. V. Fedorenko, JETP Lett. 2, 197 (1965).
[25]R. A. Mapleton and N. Grossbard, Phys. Rev. 188, 228 (1969).
[26]J. R. Hiskes, Lawrence Livermore Laboratory Report No. UCRL-50602 (1969).
[27]V. S. Nikolaev, Sov. Phys. JETP 24, 847 (1967).
[28]M. Gryzinski, Phys. Rev. 138, A336 (1965).
[29]D. N. Tripathi and D. K. Rai, Phys. Rev. A 6, 1063 (1972).
[30]Binding energies for the various subshells used in the present calculation have been taken from two sources: C. E. Moore, *Atomic Energy Levels*, Natl. Bur. Std. Circ. No. 467 (U. S. GPO, Washington, D. C., 1949); F. Herman and S. Skillman, *Atomic Structure Calculations* (Prentice-Hall, Englewood Cliffs, N. J., 1963).
[31]J. D. Garcia and E. Gerjuoy, Phys. Rev. 165, 72 (1968).
[32]Preliminary results were reported in T. J. Morgan and F. Erikson, Phys. Lett. A 66, 198 (1978). It should be noted that they do not include the high-energy correction due to competing collisions (see Sec. III).
[33]R. N. Il'in, D. A. Oparin, I. T. Serenkov, S. E. Solov'ev, and N. V. Fedorenko, in *Abstracts of Papers of the Seventh International Conference on the Physics of Electronic and Atomic Collisions*, edited by (North Holland, Amsterdam, 1971), p. 793.
[34]R. E. Olson, Phys. Lett. A 55, 83 (1975).
[35]F. W. Meyer and L. W. Anderson, Phys. Lett. A 54, 333 (1975).
[36]A. V. Vinogradov and V. P. Shevel'ko, Sov. Phys. JETP 32, 323 (1971).

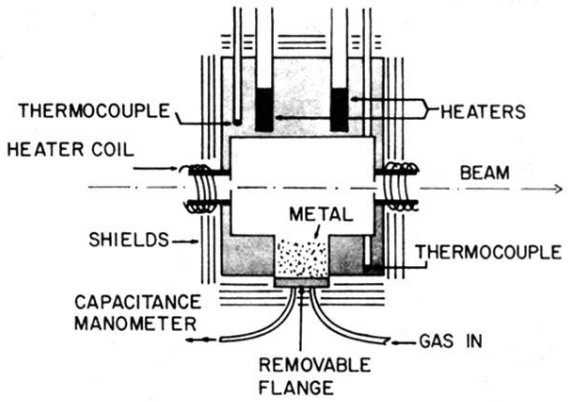


FIG. 2. Scattering target cell (not to scale). The flange containing the gas-in and pressure measuring lines was replaced by a blank flange when the cell was used as a metal-vapor target.